



HAL
open science

Estimation of two-digit grip type and grip force level by frequency decoding of motor cortex activity for a BMI application

Michele Tagliabue, Nadine Francis, Yaoyao Hao, Margaux Duret, Thomas Brochier, Alexa Riehle, Marc A Maier, Selim Eskiizmirliler

► To cite this version:

Michele Tagliabue, Nadine Francis, Yaoyao Hao, Margaux Duret, Thomas Brochier, et al.. Estimation of two-digit grip type and grip force level by frequency decoding of motor cortex activity for a BMI application. 2015 International Conference on Advanced Robotics (ICAR), Jul 2015, Istanbul, France. pp.308-315, 10.1109/ICAR.2015.7251473 . hal-04515817

HAL Id: hal-04515817

<https://hal.science/hal-04515817>

Submitted on 22 Mar 2024

HAL is a multi-disciplinary open access archive for the deposit and dissemination of scientific research documents, whether they are published or not. The documents may come from teaching and research institutions in France or abroad, or from public or private research centers.

L'archive ouverte pluridisciplinaire **HAL**, est destinée au dépôt et à la diffusion de documents scientifiques de niveau recherche, publiés ou non, émanant des établissements d'enseignement et de recherche français ou étrangers, des laboratoires publics ou privés.

Estimation of two-digit grip type and grip force level by frequency decoding of motor cortex activity for a BMI application

Michele Tagliabue¹, Yaoyao Hao², Margaux Duret², Thomas Brochier², Alexa Riehle²,
Marc A. Maier^{1,3}, Selim Eskiizmirliler^{1,3}

¹Neuroscience Research Federation FR3636, CNRS,
University Paris Descartes,
Paris, France

²Institut of Neuroscience of Timone, UMR 7289, CNRS,
University of Aix Marseille,
Marseille, France

³Department of Life Sciences,
University Paris Diderot, Sorbonne Paris Cité,
Paris, France

Abstract—This study focuses on the estimation of kinematic and kinetic information during two-digit grasping using frequency decoding of motor cortex spike trains for brain machine interface applications. Neural data was recorded by a 100-microelectrode array implanted in the motor cortex of one monkey performing reach-to-grasp movements. An artificial neural network (ANN) was used to decode the neural information and to estimate the upcoming grip type (precision grip vs. side grip) as well as the required grip force (low vs. high). We then used the decoded information to reproduce the monkey motion on a robotic platform comprised of a two-finger, eleven degrees of freedom (DoF) robotic hand carried by a six DoF robotic arm. The results show that 1) the proposed ANN model can be used for frequency decoding of multiple motor cortex spike trains with good performance for the prediction of grip type, less so for the prediction of grip force, 2) the prediction error was significantly dependent on the position of the ANN input time window associated to different stages of the grasp movement, 3) the less good performance of grasp force prediction can be improved by optimizing the neuronal population size presented to the ANN input layer on the basis of information redundancy.

Keywords — *Brain Machine Interface (BMI), Frequency decoding, Grasp, Grip force, Motor control.*

I. INTRODUCTION

As conceptually suggested by its name a Brain Machine Interface (BMI) refers to a set of hardware and software that records brain activity, decodes the activity through prediction algorithms and then controls end effectors. Thanks to promising medical applications, BMIs have recently become more visible to other scientific domains as well as to the general public, and have even raised philosophical/ethical discussions concerning its potential use in the context of human enhancement [1]. The particular benefits of decoding of neural signals and their use through a BMI in motion control of robotic arms and hands in the case of paralyzed patients has been recently demonstrated [2, 3, 4].

One well-accepted classification of BMIs is based on the non-invasive or invasive nature of the electrophysiological technique used to record neural activity. Non-invasive BMIs exploit electroencephalogram recordings (EEG) that represent

the activity of large populations of neurons in the brain with a relatively poor spatial resolution. In contrast, invasive BMIs use intracerebral neural signals like spikes or local field potentials (LFPs) recorded from single or multiple cortical areas via surgically implanted individual electrodes or multielectrode arrays (MEAs). Whatever the source of the signals, the objective is to record signals that are strongly correlated to the physical variables to be controlled by the BMI, such as kinematic variables for the control of voluntary movements [review: 5, 6]. Over the last decade, significant advances have been made on the kinematic control of reach and grasp movements [7, 8, 9], but the types of neural signals used, the choice of decoding algorithms and the dynamic control of movements of daily life remain essential problems to be solved in order to restore mobility in paralyzed and/or handicapped people.

Historically, the majority of invasive BMIs tested in non-human primates relied on the recording of local field potentials, [10] single-cell or multi-unit activity [9,11] from a single cortical area. Most of these single-area BMIs used neural signals recorded in the primary motor cortex. However, neural activity from the premotor areas [12] and the parietal cortex [13, 14] have also been used to decode movement kinematics or classified between distinct movement goals. Multi-site recordings have recently become more frequent [15, 16, 17, 18, 19]. In term of recording techniques, different types of electrodes (ceramic-based micro-electrodes, nanotechnology probes, or electrodes containing neurotrophic medium) have been tested to improve biological compatibility and long-term functionality. Safe and continuous wireless data transmission is also among the foremost problem to be solved before BMIs could be used for long-term clinical applications. Determining the number, the location (uni-site *versus* multi-site), and the types of neurons (identified *versus* non-identified), as well as the types of signals (LFP *versus* spike trains) that optimizes a BMI system for specific tasks are still open problems.

The improvement of BMI efficacy also requires the optimization of the algorithms used to decode neural activity and generate the appropriate motor commands for artificial actuators. Competing approaches have been proposed: complex linear/nonlinear algorithms [21], Artificial Neural Network

(ANN) [20] and relatively simple linear regression models [9]. Linear methods that incorporate adaptive algorithms during subject training [2] have also been proposed.

The current medical BMI applications for the substitution of paralyzed upper limbs concern principally tetraplegic patients, with the aim of using robotic arms and hands to perform reach and grasp movements for daily activities. This is currently in an experimental stage [2,3,4]. Successful kinematic control of reach movements has been demonstrated, whereas grasp movements have so far been limited to opening and closing actions of multi-finger hands driven by conventional actuators. Neither the control of different grasp configurations nor the control of grasp forces has been yet demonstrated, in spite of substantial advances in decoding cortical activity for the estimation of finger joint angles and grip forces (and/or EMGs of hand muscles) [17,20]. Therefore, the implementation of force control remains a scientific and clinically relevant research topic for BMI applications. The potential advantages of using ‘soft arms’ actuated by artificial muscles for force control might also be considered.

In our previous work [20,30], we have shown the results obtained by asynchronous temporal decoding of the activity of identified corticomotoneuronal (CM) cells recorded by individual electrodes in the primary motor cortex, while the monkey performed a precision grip task. The spike trains recorded from up to six CM cells, which project monosynaptically to motoneurons driving target muscles, were directly used as binary inputs to a time-delayed multi-layer perceptron (TDMLP) via a sliding window that scanned the time-varying neural signal in order to take into account the temporal distribution of the individual spikes. The identification as a CM cell was based on the connectivity strength of the individual neuron to a given target muscle, quantified by the presence of post-spike facilitation obtained by spike triggered averaging of that muscle EMG [24]. The TDMLP successfully estimated the time-varying positions of thumb and index finger, as well as the activity of nine forearm muscles (EMG). The estimated fingertip positions were then used to reproduce the monkeys’ hand movements on a nine DoF 2-finger artificial hand (Shadow hand).

Here, we present the results obtained by ANN-based frequency decoding of the activity of unidentified motor cortical neurons recorded using a 100-electrode MEA in a monkey while it performed two different types of grip movements at two different force levels. The "machine" part of the BMI platform now employs an extended version of the hand used in our previous work (ref.), with two more DoF providing a mobile wrist. Moreover a six DoF robotic arm carries the hand to provide both reach and grasp movements, as shown in Fig. 1.C. In addition, this new robotic setup provides the possibility of testing different types of grips and allows recording of kinematic and dynamic variables of the motion.

II. MATERIAL AND METHODS

Grasping an object involves shaping of the hand and fingers as a function of the object's physical properties, and requires adequate grasp forces to secure object manipulation. In the majority of grasp tasks the index finger and the thumb

ensure the main motion while the other three fingers act as auxiliary end effectors. An experimental setup used to characterize different types of two-digit grips including their grasp forces has been previously presented, and was used to explore the correlations between cortical activity and grasp parameters in monkeys and in humans [22, 23]. Fig. 1A and 1C show a slightly modified version of this setup for the current BMI-related work.

A. Experimental Protocol and Data acquisition

One adult female rhesus macaque (*Macaca mulatta*) was used in the experiments. The monkey, sitting in front of the experimental apparatus, was trained to perform an instructed reach-grasp-and-pull task using one hand to obtain a food reward, while her other hand was restrained (Fig.1A). The object to be grasped was a stainless steel parallelepiped (40 mm × 16 mm × 10 mm) attached to a low-friction horizontal shuttle and rotated at a 45° angle from the vertical axis. The object had to be grasped and pulled using one of two different grips: a precision grip (PG) by placing the tips of the index and the thumb on the upper and lower sides of the object, respectively, or a side grip (SG), by placing the tip of the thumb and the lateral surface of the index on the right and left sides, respectively.

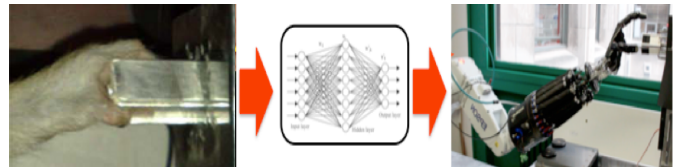


Fig. 1. Schematic representation of the offline BMI components. A) Precision and side grip experiments in monkeys. B) Decoding the cortical activity by ANN. C) End effector to reproduce the monkey motion.

The object load was set to either 100 or 200g by means of an electromagnet. Thus, two different pulling forces were required, qualified as low force (LF) or high force (HF), respectively. Changes in object load occurred between trials and were unpredictable for the monkey. The setup provided a continuous measure of the grip and load forces by means of forces sensitive resistance (FSR) sensors. In addition, a hall-effect sensor measured the horizontal displacement of the object over a maximal distance of 15mm. A square of four red light-emitting diodes (LEDs) with a fifth green LED in its center was used to display the instruction cues. The task and the recording of the physical data were programmed and controlled using LabVIEW (National Instruments Corporation, Austin, TX, USA) via an I/O card (NI PCI-6220). The behavioral sequence of a trial was as follows: the monkey had to close the home-pad switch with the hand to start a trial from the initial home-pad position. After 400ms, the central green LED was illuminated, kept on for another 400ms, and was followed by the preparatory cue, illuminated for 300ms, which instructed the monkey about the required grip type (PG or SG) followed by a 1-s preparatory delay. At the end of this delay, the LEDs provided the remaining information about the force as high force (HF) and low force (LF); this signal also served as the GO signal instructing the monkey to release the switch to reach and grasp the object. Following object grasp, the monkey had to pull the object into a narrow position (4–14mm) and to

hold it there for 500ms to obtain the reward. In case of a wrongly executed grip type, the trial was aborted and all four LEDs were flashed as a negative feedback. Several behavioral time points were defined (Fig. 3): The movement onset (taken as the time of switch release (RT), corresponding to the reaction time. The onset of grip force increase (object touch) (MT), corresponding to reach movement time. The pulling onset (PT) indicated the beginning of the object displacement. During recording sessions, the four trial types, i.e., a combination of SG-LF, SG-HF, PG-LF, and PG-HF sequences, were presented at random with equal probability.

The neural data consisted of spike trains (Fig. 2A) and LFPs (Fig. 2B) simultaneously recorded through a 4 mm × 4 mm, 100-electrodes Utah MEA (Blackrock Microsystems, Salt Lake City, UT, USA) surgically implanted in the motor cortex contralateral to the working hand, at the junction of the dorsal premotor and primary motor cortex (Fig. 2C). A 128-channel Cerebus acquisition system (Blackrock Microsystems) was used to collect and process both the neural and behavioral data, such as stimuli switch release, force traces for thumb and index fingers (Fig. 2.D) and object displacement (Fig 2.E). Here we only used the spike trains for decoding.

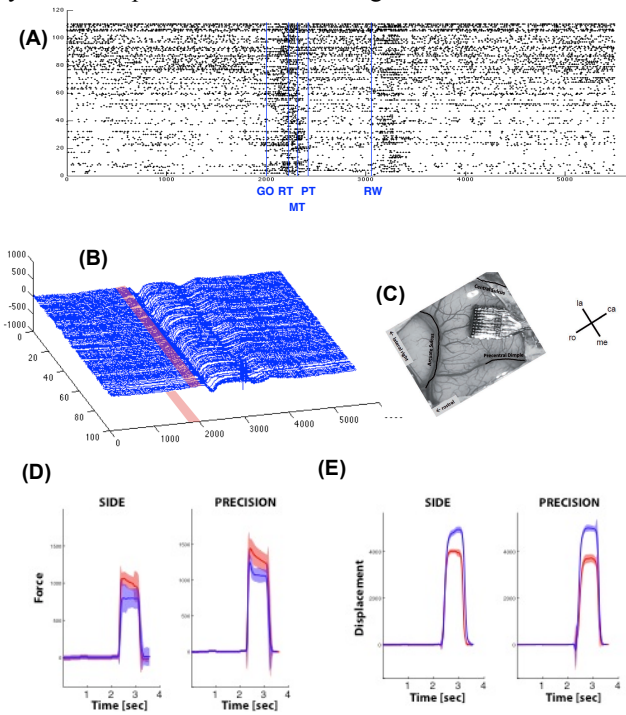


Fig. 2. Examples of neural and physical (behavioral) signals recorded during experiments. A) Raster plot of spike trains for a single trial: each line represents the neural activity of an individual neuron, with black dots indicating the presence of a spike. The vertical blue lines indicate different critical behavioral periods either detected automatically or calculated offline. GO=GO signal, RT=movement onset, MT=grip force onset., PT=pulling onset, RW=reward. B) LFPs. C) Position of the surgically implanted UTAH array. D, E) Mean and standard deviations of grip force and object displacement, respectively. Grand average of one experimental session (N=122 trials). Force and displacement are represented separately for SG (left) and PG (right) and for HF (blue lines) and LF (red lines).

Details of the data acquisition, filtering, preprocessing and spike-sorting are given in [22]. Depending on the recording session, single unit activity (SUA) was obtained from 78 to 110

neurons per recording session. Five sessions with different number of trials (19 to 34 per condition) were selected for the current decoding work.

B. ANN based frequency decoding of motor cortex activity

The way in which the central nervous system (CNS) encodes physical variables is still a partly open issue in neuroscience; this logically affects the choice in decoding approaches. Even though frequency encoding/decoding is well established and more widely studied, there is substantial evidence showing that the CNS uses also temporal distribution of spike trains in encoding physical variables [20].

The current work analyzes the performance of ANNs in frequency decoding of motor cortical activity to estimate kinematic and dynamic parameters of grasp movements. This approach differs from our previous work (ref) in the following aspects:

1. The neural data were obtained from unidentified neurons of the motor cortex and not from identified CM cells as in [ref].
2. The number of simultaneously recorded neurons (SUA) was much higher (between. 75 and. 110) due to the MEA.
3. The data preprocessing (prior to the training of the ANN) has been designed to calculate frequency discharge of each SUA over a fixed time window. The time windows were assigned to different behavioral epochs (chosen by the user). Depending on the training type, the average discharge frequency calculated within one or more time windows, was used as inputs of the ANN input neurons.
4. The outputs to be estimated by the ANN were discrete, that is the grip type (either SG or PG) and force level (either HF or LF).

Fig. 3 shows a schematic representation of the ANN architecture used for decoding. It has two layers both constituted by units with symmetric sigmoid transfer functions and bias inputs.

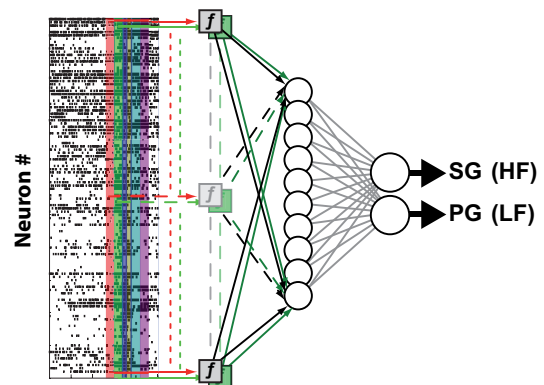


Fig. 3. Schematic representation of the ANN used in prediction of grip type (SG and PG) or load force (HF and LF) by frequency decoding of motor cortex activity. The colored regions on the raster plot represent the time windows where the average discharge frequency of each SUA (depicted by the grey square) was calculated. Green squares depict use of multiple time windows.

The input layer receives the frequency discharge calculated on the fixed time window for each SUA, whereas the two units of the output layer are dedicated to estimate the kinematic (grip type: SG and PG) or dynamic (load force: HF and LF) parameters of the movement.

Separate ANNs were designed for each of the output pairs for predicting grip type or load force using the Matlab Neural Network Toolbox. ANNs were trained and tested separately for each of the five sessions. The training trials were randomly chosen among 50% of all trials and the remaining ones were used as test trials in order to calculate the performance measure of the prediction as percentage error (%error). This procedure was repeated 30 times per session and the %error for a given session was calculated as the mean of %error obtained during those 30 training / testing epochs.

We first trained all ANNs on six different time windows of different lengths located with respect to the five critical points of the movement, as described in Table 1 and depicted in Fig. 3. The weights between the input and output layer and the bias values were initialized with Nguyen Widrow algorithm and a scaled conjugate backpropagation learning algorithm (Levenberg – Manquard backpropagation) was used to update both weights and bias values.

TABLE 1. Description of input window length and position for calculating SUA average discharge frequency.

Window	Time interval	Corresponds to:
W1	from GO-200ms to GO	Pre load-cue period
W2	from GO to RT	Reaction time period
W3	from RT to MT	Reach duration
W4	from MT to PT	Grip force increase
W5	from PT to PT+200ms	Object displacement
W6	from PT+200ms to PT+400ms	Static hold

We further checked the impact of two training parameters on the ANN performance of prediction.

1. The number of time windows used as inputs.
2. The number of SUA in a given time window. The number of inputs can be reduced by using two optimization criteria:
 - a. Removing neurons whose activity is cross-correlated (CC) to other neurons.
 - b. Removing neurons for which the Cohen's index [29], described in Fig.4, is smaller than a threshold value.

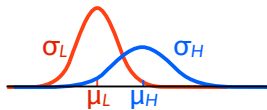
$$\text{Cohen's index} = \frac{(\mu_L - \mu_H)}{\sqrt{\sigma_L^2 + \sigma_H^2}}$$


Fig. 4. Calculation of the optimization criterion, where μ and σ represent respectively the mean and the standard deviations of the discharge frequency calculated over the trials corresponding to a given experimental condition.

C. Reproduction of the motion on the robotic platform

Fig. 5 shows the current state of our BMI platform. It consists of three main modules:

1. A copy of the experimental reach-grasp-and-pull setup used by the monkey, described in section II.A. The size of the parallelepiped is, however, bigger (60 mm × 40 mm × 30 mm) in order to fit the size of the Shadow (and of the human) hand.
2. A 6 DoF robotic arm (@Epson S5)
3. A 11 DoF 2-finger robotic hand actuated by artificial muscles (@Shadow Hand).

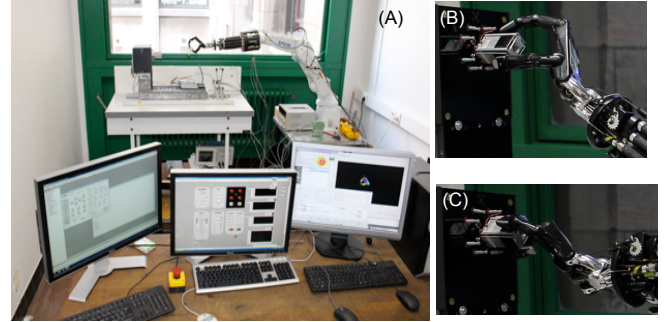


Fig. 5. A) Current state of the BMI platform. B) Precision grip with the robotic hand. C) Side grip with the robotic hand.

Each of the three modules is controlled by a separate personal computer (PC), and the whole system is centrally controlled by a custom BMI software installed on the PC controlling the Shadow Hand, which exchanges information with the PCs of the two other modules via either serial or Ethernet ports connected to a router. The BMI software using the neural data as input controls the reach motion (positioning) of the hand driven by the 6 DoF robotic arm and selects the corresponding ANN, whose prediction is used to drive the grasp motion of the hand.

Due to the lack of joint angle recordings in the monkey, the motion parameters of the reach and the grasp were manually set so that SG or PG and subsequent pulling were executed as shown in Fig. 5, B and C. In order to realize two different grip forces, the surface of the grasp object was coated with compressible foam strips (of 3cm thickness).

III. RESULTS

Training of the ANNs resulted in error values < 0.1% on the training set. In the following we report the %error on the test set (median %error over 5 sessions per condition).

Fig. 6 shows, from top to bottom, examples of behavioral and neural data from a representative trial and the evolution of average percentage prediction errors of the ANNs for grip type and load force decoding as a function of 6 different time windows (cf Table 1) calculated over five sessions. Clearly, the %error of the prediction varied as a function of the position of the time window and of the condition. This was confirmed by nonparametric Friedman ANOVA showing that the percentage error was significantly affected by the time window position in predicting grip type [$\chi^2(5,5)=16.28, p=0.006$] and in predicting load force [$\chi^2(5,5)=18.49, p=0.002$]. The error decreased continuously from W1 to W5, and then increased at W6. In predicting grip type, the median percentage error was equal to 2% for W2 to W5, with a best performance on W5; it was 4% for W1, a window prior to movement onset, which represents

anticipatory activity. The error increased to 7% for W6, a window that covers the period of static hold against the load.

In contrast, the performance of load force prediction was dramatically lower. At W1, prior to the GO signal, %error was about 50%, corresponding to chance prediction. This served as a control, since no load instruction was given prior to GO. The error then decreased steadily from W2 on and reached its minimum with 25% error at W5. Thus, W5 provided the best prediction, for grip type and for load force. W5 represents the period from touch onset to the end of the displacement: during this period the grip type is firmly established and invariant, whereas grip force and load force change over time.

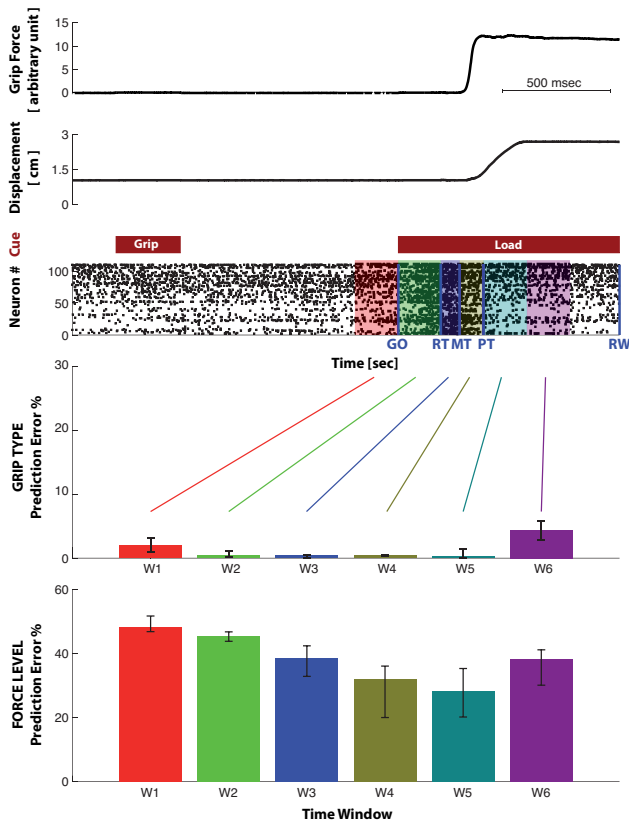


Fig. 6. Effect of six different positions of the neural input time window on the performance of ANN prediction of grip type and load force. From top to bottom (first three panels): example of a representative trial with grip force, object displacement (pulling) and raster plot of a neural data. In color and superposed to the raster plot: the positions of the 6 different input time windows. Below: median %error (across all 5 sessions) of grip type prediction for each input time window. median %error (across all 5 sessions) of load force prediction for each input time window; the whisker bars correspond to the 25th and 75th percentiles.

Since performance of load force prediction was as not good as grip type prediction, we investigated whether input optimization would improve the former. We first evaluated the effect of combining several (from 2 up to 4) input windows. These results are represented in Figure 7. A Friedman ANOVA showed that the number of combined windows has a significant effect on the %error of load force prediction [$\chi^2(5,3)=15.00, p=0.0018$], with a best result for the combination of four windows.

Second, we evaluated the effect of reducing (optimizing) the number of neurons in a given time window by eliminating redundant SUA according to criteria described in section II.B (cross-correlation, Cohen’s Index). Table 2 reports the %errors and the amount of removed neurons as a function of the corresponding threshold values obtained by separate application of the two criteria. The first line of Table 2 gives the reference values corresponding to the performance of prediction obtained without optimization.

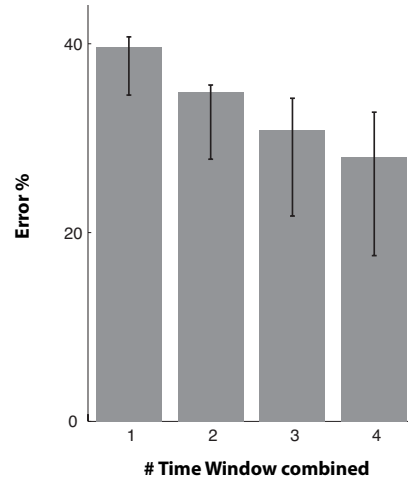


Fig. 7. Effect of combining several time windows on the median prediction error of load force. 1: no combination, %error of 6 ANNs trained using the neural data on each of the single windows defined in table 1. 2: combination of two windows, average error of 5 ANNs using combinations of two windows. 3: combination of 3 windows, %error of 4 ANNs using combinations of three windows. 4: combination of four windows.

The threshold of Cohen’s index (first column Table 2) was systematically varied and neurons with an index greater than the threshold were kept. For the second optimization criterion neurons with cross-correlation smaller than the threshold were kept. Application of Cohens’s index was more efficient: it strongly reduced the number of input neurons (76%) and improved the load force prediction (%error decreased from 24.35% to 18.73%). The cross-correlation procedure allowed for only modest improvements of prediction accuracy and the combined use of both optimization criteria (Cohen’s index > 0.9 and CC < 0.8) did not improve the performance any further (19.16 %error with 76% removed neurons).

TABLE 2. Effect of the reduction of the number of input neurons (best case in red).

Cohen’s index	Error	% Neurons removed	Cross-corr threshold	Error	% Neurons removed
0	24.35	0	1	24.35	0
0.95	19.60	79	0.9	24.38	0
0.9	18.73	76	0.85	23.95	1
0.8	19.48	62	0.8	23.40	4
0.7	19.76	49	0.7	25.20	21
0.6	19.97	34	0.6	26.44	39
0.5	21.56	17	•	•	•
0.4	23.53	7	•	•	•

For evaluation of the robotic part for our offline BMI application, we used best-case predictions. The ANN using the

neural data in W5 was the best predictor for grip type. For load force prediction, we used the ANN trained on the combination of several windows (W1, W2, W3, W4), including optimization through Cohen's index > 0.9 (using 24% of the original neurons). Then the weights of these two trained ANNs were transferred to the ANN part of the main control software of the BMI platform to perform an offline BMI test. Due to the lack of empirical joint angle values from the monkey experiments, we manually defined four different joint configurations of the shadow hand to realize four different movement conditions (as defined above in section II.A). Figure 8 shows the force traces obtained for SG-HF and SG-LF experiments realized on the "machine" part of the BMI platform with the joint values reported in Table 3.

TABLE 3. The Shadow hand joint angles corresponding to two joint configurations for side grip with two different force levels. IF_J=Index Finger Joint; TH_J=Thumb_Joint. J1 corresponds to the most distal, J4 and J5 to the most proximal joints of the index and thumb, respectively.

Shadow hand joints	SG-LF	SG HF
IF J1	75	75
IF J2	85	85
IF J3	90	90
IF J4	0	20
TH J1	30	51
TH J2	18	21
TH J3	-15	-15
TH J4	60	70
TH J5	40	20

Clearly, the robot hand applies higher thumb and index finger forces in the HF-condition compared to the LF-condition. Note that the speed of the movement (force production) is slower than in the monkey (c.f. Fig. 6A).

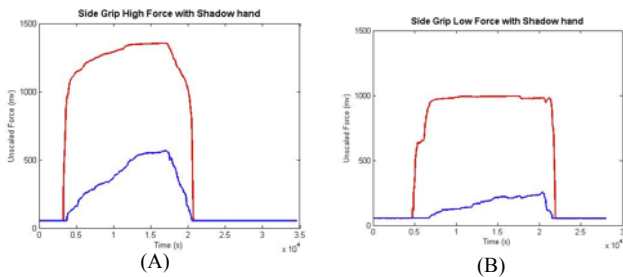


Fig. 8. Forces exerted on the object surfaces by the thumb (blue line) and index finger (red line) of the Shadow hand using two different joint configurations corresponding to two different force levels. A) Side grip with high force. B) Side grip with low force.

IV. CONCLUSIONS

Here we presented a BMI platform to reproduce upper limb reach-grasp-and-pull movements using a two-digit grasp. Neural data were obtained from the monkey motor cortex. The monkey was instructed to perform a reach, grasp an object with either a precision grip or a side grip, and then pull the object against a either high or low load. In contrast to our previous work [20], which presented the results of temporal decoding of identified CM cells, frequency decoding of

spiking neural activity of unidentified primary cortex neurons was achieved by a two-layer ANN that predicted grip type (precision grip vs. side grip) and load force (high and low). A 11-DoF artificial hand carried by a 6- DoF robotic arm was used to reproduce the upper limb movement.

The ANN (using time windows of variable positions within a behavioral trial, defined in Table 1 provided reliable prediction of grip type, whereas prediction of load force was less good as shown in Fig. 6. Therefore, grip type information can be decoded with high accuracy from multiple spike trains during the preparatory period (W1), during the reaction time period before movement onset (W2), as well as during movement execution (W3-W5). This has been shown previously, for more than two grip types, however, with other methods than ANNs [24, 12, 17]. During static hold, prediction accuracy was worst. Qualitatively, the firing rate (and tentatively the amount of information) tended to increase after the GO signal and decreased to initial levels during static hold.

In contrast, load force decoding was more difficult: best %error of load prediction was, compared to grip type prediction, larger by a factor of ten. Although this may indicate that the grip force cannot be reliably decoded under the current experimental situation, there are several arguments in favor of such a decoding. First, the ANNs decoded load force perfectly fine for the training trials. However, for the test trials the %error increased dramatically. This suggests that load information was not sufficiently robust in the face of behavioral trial-to-trial variability and neural noise. Second, this interpretation is coherent with anecdotic evidence (not shown) that the accuracy of load prediction increases with better behavioral performance, i.e. with better differentiation between low and high forces. However, this needs to be statistically confirmed on a larger data set. Under different behavioral situations, endpoint force decoding [26] and whole-hand grasp force decoding from spike trains has been demonstrated [27]. Other speculative reasons for the poor load decoding might reside in the location of the MEA (rather dorsal, junction premotor-primary motor cortex, but this needs further investigation) and in the absence of explicit (visual) force feedback to the monkey.

Even though it has been suggested that recording more signals will mean higher accuracy [18] and better performance (dexterity) [ref], there is evidence that BMI systems using a small number of neurons could also be quite competitive [20, 28]. Redundant information in the input layer constitutes one of the well-known drawbacks of ANN approach in prediction of small number of outputs from a large number of inputs. Our results of selecting the inputs (Fig. 7) constitute a good example: prediction of load force was significantly improved by optimizing the input, even though performance remained well below that of grip type decoding. Optimization by using a criterion based on Cohen's index (depth of firing rate modulation) proved to be more efficient than taking into account cross-correlations (temporal redundancy in multiple

spike trains (Table 2). This is coherent with the fact that our ANNs used frequency and not temporal decoding.

In general, accuracy of prediction depended significantly on the position of the time window during different epochs of the task. Best decoding (using a single window) was achieved in W5, for grip as well as for load force. W5 covered the period from touch onset to the end of the displacement, i.e. during object contact with stable grip type, while grip and load force varied (increased). This suggests that kinematic prediction accuracy is best once the kinematic grip configuration is established, although anticipatory decoding during reaction time and during reach (grip preshaping) was smaller by only a marginal amount. In contrast, accuracy of load force prediction increased from W2 and reached a maximum during W4 and W5, i.e. during periods of object contact when grip force increases (W4) and when load force increases (W5). This tentatively suggests that force decoding is most efficient during active production of (grip or load) forces. This conclusion must, of course, be taken with caution since the grip type cue was given first, and the force cue only later, which might have biased this comparison.

The end-effector of the BMI platform used here was a 2 finger artificial hand actuated by pneumatic muscles (Shadow muscle hand) carried by a 6 DOF robotic arm (Epson S5). The Shadow hand has an anthropomorphic actuation scheme providing movement of the distal interphalangeal (DIP) joint of the index finger coupled to that of the proximal interphalangeal (PIP) joint. The kinematic control of the joint angles is implemented by a PID position controller that adjusts the pressure of compressed air in each pneumatic muscle until the desired angles are reached. As long as the joint angles are not at their target values, the PID position controller increases the pressure of the pneumatic muscles up to their maximum values and thus generates a grasp with a maximal force. This excludes implementation of any force control in joint space for isometric grips i.e. testing different force levels for a given static joint configuration, similar to what the monkey did in low and high load conditions, was therefore impossible.

In the aim of testing the capacity of the Shadow hand in implementing a force control in joint space, we conducted several experiments of different grip types at different force levels with the grasp object coated with compressible foam strips (of 3cm thickness) on each of its surfaces. As can easily be seen on the values reported in Table 3 and the forces shown in Fig. 8 for the SG experiments two significantly different and stable force levels (HF and LF) were successfully obtained with two different and stable joint configurations. These results can potentially be further improved by adding a PID or 'sliding mode' control of muscle pressure. This strategy could be used as an alternative to the position controller, once the grasp configuration has been established in order to provide co-contraction of the muscles. However, this should only be considered a preliminary solution to the force control problem of future BMI applications, which need to implement the simultaneous control of kinematics and dynamics, as does the central nervous system.

ACKNOWLEDGMENT

The authors would like to thank Dr. Ivan Balansard for the surgical operation and Mr. Xavier Degiovanni, Mr. Joël Baurberg, Mr. Patrice Jegouzo, Mr. Christophe Tourain for the design and fabrication of the mechanics and electronics of the experimental setups and Ms. Nadine Francis for the experiments with the shadow hand.

- [1] S. Eskiizmirliler and J. Goffette, "BMI (Brain-Machine Interface) as a tool for understanding human-machine cooperation," in *Human Enhancement: an interdisciplinary inquiry*, S. Bateman, J. Gayon, S. Allouche, J. Goffette, M. Marzano, Eds. London: Palgrave MacMillan, in press.
- [2] L.R. Hochberg, et al. "Reach and grasp by people with tetraplegia using a neurally controlled robotic arm," *Nature* 2012, 485:372-375.
- [3] J.L. Collinger, et al. "High-performance neuroprosthetic control by an individual with tetraplegia," *Lancet*. 2013 Feb 16;381(9866):557-64.
- [4] T. Yanagisawa, et al. "Real-time control of a prosthetic hand using human electrocorticography signals," *J Neurosurg* 2011; 114: 1715-22.
- [5] M.A.L. Nicolelis, M.A. Lebedev, "Principles of neural ensemble physiology underlying the operation of brain-machine interfaces," *Nature Rev. Neurosci.* 2009, 10: 530-540.
- [6] R. Héliot and J.M. Carmena, "Brain-Machine Interfaces", *Encyclopedia of Behavioral Neuroscience*, 2010, 221-5.
- [7] J. Wessberg, et al. "Real-time prediction of hand trajectory by ensembles of cortical neurons in primates," *Nature*, 2000, 408, 361-5.
- [8] M.A. Lebedev, et al. "Cortical ensemble adaptation to represent velocity of an artificial actuator controlled by a brain-machine interface," *Journal of Neuroscience*, 2005, 25(19), 4681-93.
- [9] M. Velliste, S. Perel, M.C. Spalding, A.S. Whitford, A.B. Schwartz, "Cortical control of a prosthetic arm for self-feeding," *Nature*, 2008 Jun 19;453(7198):1098-101.
- [10] Rickert J. et al. "Encoding of movement direction in different frequency ranges of motor cortical local field potentials," *Journal of Neuroscience*, 2005, 25, 8815-24.
- [11] J.M. Carmena et al. "Learning to control a brain-machine interface for reaching and grasping by primates," 2003, *PLoS Biology*, 1, 193-208.
- [12] B.R. Townsend, E. Subasi and H. Scherberger, "Grasp Movement Decoding from Premotor and Parietal Cortex," *The Journal of Neuroscience*, October 5, 2011, 31(40):14386-14398.
- [13] S. Musallam, B.D. Corneil, B. Greger, H. Scherberger, R.A. Andersen, "Cognitive control signals for neural prosthetics," *Science*, 2004 Jul 9;305(5681):258-62.
- [14] H. Scherberger, M.R. Jarvis, R.A. Andersen, "Cortical local field potential encodes movement intentions in the posterior parietal cortex," 2005, *Neuron* 46:347-354.
- [15] J. Wessberg et al. "Real-time prediction of hand trajectory by ensembles of cortical neurons in primates," *Nature*. 2000 Nov 16;408(6810):361-5.
- [16] R.A. Andersen, H. Cui, "Intention, action planning, and decision making in parietal-frontal circuits," *Neuron*, 2009 Sep 10;63(5):568-83.
- [17] S. Schaffelhofer, A. Agudelo-Toro, H. Scherberger, "Decoding a wide range of hand configurations from macaque motor, premotor, and parietal cortices," *J Neurosci.* 2015 Jan 21;35(3):1068-81.
- [18] D.A. Schwarz, MA Lebedev, TL Hanson, DF Dimitrov, G Lehew, J. Meloy S Rajangam, V Subramanian, PJ Ifft, Z Li, A Ramakrishnan, A Tate, KZ Zhuang, MA Nicolelis. "Chronic, wireless recordings of large-scale brain activity in freely moving rhesus monkeys," *Nat Methods*. 2014 Jun;11(6):670-6.
- [19] A.K. Bansal, C.E. Vargas-Irwin, W. Truccolo, J.P. Donoghue, "Relationships among low-frequency local field potentials, spiking activity, and three-dimensional reach and grasp kinematics in primary motor and ventral premotor cortices," *J Neurophysiol.* 2011 Apr;105(4):1603-19.
- [20] S. Ouanezar, S. Eskiizmirliler, M.A. Maier, "Asynchronous decoding of finger position and of EMG during precision grip using CM cell activity: application to robot control," *J Integr Neurosci* 2012, 10(4):489-511.

- [21] E.N. Brown, R.E Kass, P.P. Mitra 'Multiple neural spike train data analysis: state-of-the-art and futur challenges', *Nature Neuroscience*, - 2004, 7(5), 456-61.
- [22] A. Riehle, S. Wirtsohn, S. Grün, T. Brochier. Mapping the spatio-temporal structure of motor cortical LFP and spiking activities during reach-to-grasp movements. *Front Neural Circuits*. 2013 Mar 27;7:48.
- [23] M. Zaepffel, R. Trachel, B.E. Kilavik, T. Brochier, "Modulations of EEG Beta Power during Planning and Execution of Grasping Movements," 2013, PLoS ONE 8(3): e60060. doi:10.1371/journal.pone.0060060.
- [24] M.A. Maier, K.M. Bennett, M.C. Hepp-Reymond and R.N. Lemon, "Contribution of the monkey corticomotoneuronal system to the control of force in precision grip," 1993, *J. Neurophysiol.* , 69 , 772_ 785.
- [25] M.A. Umilta, T. Brochier, R.L. Spinks, R.N. Lemon, "Simultaneous recording of macaque premotor and primary motor cortex neuronal populations reveals different functional contributions to visuomotor grasp," *J Neurophysiol*. 2007 Jul;98(1):488-501.
- [26] R. Gupta, J. Ashe, "Offline decoding of end-point forces using neural ensembles: application to a brain-machine interface," *IEEE Trans Neural Syst Rehabil Eng*. 2009 Jun;17(3):254-62.
- [27] C. Ethier, E.R. Oby, M.J. Bauman, L.E. Miller, "Restoration of grasp following paralysis through brain-controlled stimulation of muscles," *Nature*. 2012 May 17;485(7398):368-71.
- [28] C.E. Vargas-Irwin, G. Shakhnarovich, P. Yadollahpour, J.M. Mislaw, M.J. Black, J.P. Donoghue, "Decoding complete reach and grasp actions from local primary motor cortex populations," *J Neurosci*. 2010 Jul 21;30(29):9659-69.
- [29] J. Cohen, "Statistical power analysis for the behavioural sciences", 1988 (2nd ed.). Hillsdale, NJ: Erlbaum.
- [30] S. Eskiiizmirli, O. Bertrand , M. Tagliabue, M.A. Maier, "Motion control of thumb and index finger of an artificial hand for precision grip using asynchronous decoding of CM cell activity," *BMC Neuroscience* 2013, 14(Suppl 1):P254, CNS 2013, June 13-18, Paris,